Quaternary Science Reviews 29 (2010) 222–234

Contents lists available at ScienceDirect

Quaternary Science Reviews

journal homepage: www.elsevier.com/locate/quascirev

Synchronising EDML and NorthGRIP ice cores using $\delta^{18}O$ of atmospheric oxygen ($\delta^{18}O_{atm}$) and CH_4 measurements over MIS5 (80–123 kyr)

E. Capron[a,*], A. Landais[a], B. Lemieux-Dudon[b], A. Schilt[c], V. Masson-Delmotte[a], D. Buiron[b], J. Chappellaz[b], D. Dahl-Jensen[d], S. Johnsen[d], M. Leuenberger[c], L. Loulergue[b], H. Oerter[e]

[a] Institut Pierre-Simon Laplace/Laboratoire des Sciences du Climat et de l'Environnement, CEA-CNRS-UVSQ, 91191 Gif-sur-Yvette, France
[b] Laboratoire de Glaciologie et Géophysique de l'Environnement, CNRS-UJF, 38400 St Martin d'Hères, France
[c] Climate and Environmental Physics, Physics Institute, and Oeschger Centre for Climate Change Research, University of Bern, Sidlerstrasse 5, CH-3012 Bern, Switzerland
[d] Department of Geophysics, Julianes Maries Vej 30, University of Copenhagen, 2100 Copenhagen, Denmark
[e] Alfred Wegener Institute for Polar and Marine Research, Bremerhaven, Germany

A R T I C L E I N F O

Article history:
Received 12 December 2008
Received in revised form
20 July 2009
Accepted 22 July 2009

A B S T R A C T

Water isotope records from the EPICA Dronning Maud Land (EDML) and the NorthGRIP ice cores have revealed a one to one coupling between Antarctic Isotope Maxima (AIM) and Greenland Dansgaard-Oeschger (DO) events back to 50 kyr. In order to explore if this north–south coupling is persistent over Marine Isotopic Stage 5 (MIS 5), a common timescale must first be constructed.

Here, we present new records of $\delta^{18}O$ of O_2 ($\delta^{18}O_{atm}$) and methane (CH_4) measured in the air trapped in ice from the EDML (68–147 kyr) and NorthGRIP (70–123 kyr) ice cores. We demonstrate that, through the period of interest, CH_4 records alone are not sufficient to construct a common gas timescale between the two cores. Millennial-scale variations of $\delta^{18}O_{atm}$ are evidenced over MIS 5 both on the Antarctic and Greenland ice cores and are coupled to CH_4 profiles to synchronise the NorthGRIP and EDML records. They are shown to be a precious tool for ice core synchronisation.

With this new dating strategy, we produce the first continuous and accurate sequence of the north–south climatic dynamics on a common ice timescale for the last glacial inception and the first DO events of MIS 5, reducing relative dating uncertainties to an accuracy of a few centuries at the onset of DO events 24 to 20. This EDML-NorthGRIP synchronisation provides new firm evidence that the bipolar seesaw is a pervasive pattern from the beginning of the glacial period. The relationship between Antarctic warming amplitudes and their concurrent Greenland stadial duration highlights the particularity of DO event 21 and its Antarctic counterpart. Our results suggest a smaller Southern Ocean warming rate for this long DO event compared to DO events of MIS 3.

1. Introduction

Since its discovery in Greenland ice cores (Dansgaard et al., 1984) the millennial climatic variability of the last glacial period has been increasingly documented at all latitudes (e.g. Voelker, 2002; Wang et al., 2008). Ice core records from Greenland and Antarctica have revealed the phase relationships between the Dansgaard-Oeschger events (hereafter DO events) recorded in the Northern Hemisphere and their Southern counterparts, the so-called Antarctic Isotope Maxima (AIM) (Bender et al., 1994; Jouzel et al., 1994; Blunier et al., 1998; Bender et al., 1999; Blunier and Brook, 2001; EPICA community members, 2006). The Antarctic temperature as recorded by the water isotopes increases slowly during cold Greenland stadials. This bipolar seesaw is understood to reflect the impact of the north–south heat redistribution through thermohaline circulation changes and thermal inertia of the Southern Ocean (Stocker and Johnsen, 2003; Knutti et al., 2004).

The aforementioned studies mainly concentrated on the sequence of events during MIS 2 and 3, from the middle of the last glacial period to the deglaciation, when DO events are relatively short and frequent (i.e. 17 DO events between 60 and 10 kyr). By contrast, DO events are less frequent during MIS 4 and 5 (i.e. 8 DO events between 110 and 60 kyr) and only one study presents a work going back to DO event 21 (Blunier and Brook, 2001). It is of primary importance to characterise the bipolar structure of millennial-scale variability at its onset, during the glacial inception, i.e. at a period with small ice sheet extent (−40 m sea level relative to present; Waelbroeck et al., 2002; Bintanja et al., 2005)

* Corresponding author. Tel.: +33 169082702; fax: +33 169087716.
E-mail address: emilie.capron@lsce.ipsl.fr (E. Capron).

0277-3791/$ – see front matter © 2009 Elsevier Ltd. All rights reserved.
doi:10.1016/j.quascirev.2009.07.014

as well as the climate dynamics during the long DO events 19, 20 and 21 of MIS 4–5. This requires a reliable Greenland ice core record extending back to MIS 5. The recently drilled NorthGRIP ice core (75.10 °N, 42.32 °W, 2917 meters above sea level (m a.s.l.), 17.5 cm w. e. yr^{-1}, NorthGRIP-community-members, 2004) now provides an undisturbed record of the past 123 kyr (NorthGRIP-community-members, 2004) with the opportunity to establish an absolute timescale based on layer counting for the entire glacial period. The Greenland Ice Core Chronology (GICC05) is now available for the last 60 kyr (Svensson et al., 2008). Thanks to limited thinning, the NorthGRIP ice core provides a high resolution reference for climatic variability at the very beginning of the last glacial period including the first DO event 25.

Identifying sequences of events requires a common and precise Greenland/Antarctic ice core timescale that can be obtained through global atmospheric tracers such as isotopic composition of atmospheric oxygen, $\delta^{18}O$ of O_2 and methane (in the following, $\delta^{18}O_{atm}$ and CH_4 respectively; Blunier et al., 1998; Blunier and Brook, 2001; EPICA community members, 2006; Blunier et al., 2007). The $\delta^{18}O_{atm}$ signal is a complex signal integrating changes of the global ice volume (Sowers et al., 1993), biosphere productivity and hydrological cycle (Bender et al., 1994; Leuenberger, 1997; Severinghaus et al., 2009; Landais et al., 2010). Atmospheric CH_4 concentration responds very fast to a change in the production of CH_4 and so, abrupt Greenland DO warmings are associated with sharp CH_4 rises within 50 yr (Chappellaz et al., 1993; Severinghaus et al., 1998; Flückiger et al., 2004; Huber et al., 2006). Nitrogen isotopes measured in the air trapped in the ice can be used as a complementary tool to identify the onset of DO events directly in the gas records of Greenland ice cores (Severinghaus et al., 1998; Blunier and Brook, 2001; Landais et al., 2004; Huber et al., 2006).

After an initial attempt based on the use of nitrogen and argon isotopes and limited to DO event 24 (Caillon et al., 2003), a first common dating of Antarctic (Vostok) and Greenland (NorthGRIP) ice cores over MIS 5 has been constructed using $\delta^{18}O_{atm}$ measured in air trapped in ice (Landais et al., 2006b). Within age scale uncertainties, DO events 23 and 24 were suggested to exhibit a north/south seesaw behaviour. This study was not fully conclusive on the DO event 25 which has no apparent counterpart in the Vostok δD profile. However, these analyses were limited by several key points. First, the north–south correlation was built through low resolution records of $\delta^{18}O_{atm}$ (1500 yr in Vostok) leading to large uncertainties in the determination of tie points (1000–2500 yr); second, the surface characteristics of the Vostok site (low accumulation rate – 2.2 cm water equivalent (w.e) yr^{-1} and temperature – −55 °C) limit the detection of Antarctic events in the water isotopic profile despite the 100 yr resolution of the measurements (Petit et al., 1999); third, these extreme surface conditions of the Vostok site lead to a strong age difference between ice and gas at the same depth, hereafter noted Δage, reaching up to 5000 yr with a 20% uncertainty and thus contributing to a large uncertainty in the north–south synchronisation of the water isotopic records.

The EPICA Dronning Maud Land (hereafter noted as EDML – 75.00°S, 0.07°E, 2882 m a.s.l., 6.4 cm w.e.yr^{-1}, EPICA community members, 2006) ice core has been recently retrieved in the Atlantic sector of East Antarctica. Because of its relatively high accumulation rate and temperature, it allows increasing the temporal resolution with respect to Vostok. Moreover, the EDML Δage is estimated to be less than 2000 yr, i.e. 2–3 times smaller than at central Antarctic sites such as Vostok or Dome C (Loulergue et al., 2007). The current EDML1 ice chronology (Ruth et al., 2007) has been derived by synchronising the EDML and EPICA Dome C (EDC) ice core records on the EDC3 glaciological age scale (the EDC3 age scale is described in Parrenin et al., 2007), using volcanic horizons and dust peaks (Severi et al., 2007).

In this paper, we present in Section 2, available and new high resolution (̃100 yrs) records of CH_4, $\delta^{18}O_{atm}$ and $\delta^{15}N$ over MIS 4 and 5 on the NorthGRIP and EDML ice cores and highlight significant millennial-scale variability in the EDML $\delta^{18}O_{atm}$ record. In Section 3, we describe our methodology to infer tie points between the NorthGRIP and EDML gas records from the combined measurements of CH_4 and $\delta^{18}O_{atm}$. We emphasize the added value of high resolution $\delta^{18}O_{atm}$ records for this synchronisation. The uncertainty associated with the EDML Δage calculation is then discussed. Finally, we propose a common timescale for EDML and NorthGRIP gas records based on the EDML1 chronology as a reference (Ruth et al., 2007). We improve the accuracy of the north–south synchronisation of water isotopic records and this permit to discuss the north–south sequence of the rapid climate variability in the first part of the last glacial period (Section 4).

2. Data

2.1. CH_4 measurements

CH_4 measurements were conducted at Laboratoire de Glaciologie et Géophysique de l'Environnement (LGGE, Grenoble) and at the University of Bern. The analytical methods of CH_4 measurements are detailed in Spahni et al. (2005) and Loulergue et al. (2008). They lead to a 10-ppbv mean measurement uncertainty (Chappellaz et al., 1997). We present the first CH_4 measurements performed over the bottom part of the NorthGRIP ice core: 150 samples from the NorthGRIP ice core over the depth range 2276–3084 m (1 m depth resolution) were analysed. CH_4 concentrations vary from 757 to 450 ppbv and cover the time interval between the last glacial inception and DO event 23 (Fig. 1). Combining 160 samples analysed at LGGE with the 112 measurements conducted at Bern on the EDML ice core, the mean depth resolution is about 2 m for the EDML CH_4 record over the depth range 1828–2394 m.

Based on the official gas timescale published in Loulergue et al. (2007), the EDML CH_4 profile offers a record with mean temporal resolution of 190 yr, comparable to the 210 yr average resolution for EDC (Loulergue et al., 2008). The glacial inception is clearly visible as a steady regular CH_4 decrease from 725 ppbv to 448 ppbv as well as the fluctuations linked to DO events already shown in several Antarctic ice cores (e.g. Byrd station, Blunier et al., 1998; Blunier and Brook, 2001; EDC, Loulergue et al., 2008; Fig. 1).

2.2. $\delta^{18}O_{atm}$ and $\delta^{15}N$ measured in the air trapped in the ice: analytical procedure and results

The isotopic and elementary compositions of trapped air ($\delta^{15}N$, $\delta^{18}O$, $\delta O_2/N_2$) have been measured at Laboratoire des Sciences du Climat et de l'Environnement (LSCE). To complete the high resolution NorthGRIP $\delta^{18}O_{atm}$ data sets published in Landais et al. (2007) and Landais et al. (2006b) over DO events 18, 19, and 20 (1–2 m resolution), DO events 23, 24 (1–2 m resolution) and 25 (5 m resolution) respectively, additional measurements were performed over DO events 21, 22 and 25 on 215 depth levels (1 m resolution). On the EDML ice core, measurements are reported from 145 depth levels between 1829 and 2426 m, i.e. covering MIS 4 and 5, with a 4 m resolution. Published $\delta^{18}O_{atm}$ and $\delta^{15}N$ measurements (Landais et al., 2004, 2006b, 2007) used a manual melt refreeze air extraction technique combined with isotopic ratio measurements on a MAT 252 (Finnigan) (see Landais et al., 2003 for analytical procedure). New measurements have been performed using an automated melt extraction technique of air with water trapped at −90 °C. Samples were then analysed with a Delta V Plus (ThermoElectron Corporation) mass spectrometer. Results are reported with respect to atmospheric air. Corrections for pressure imbalance

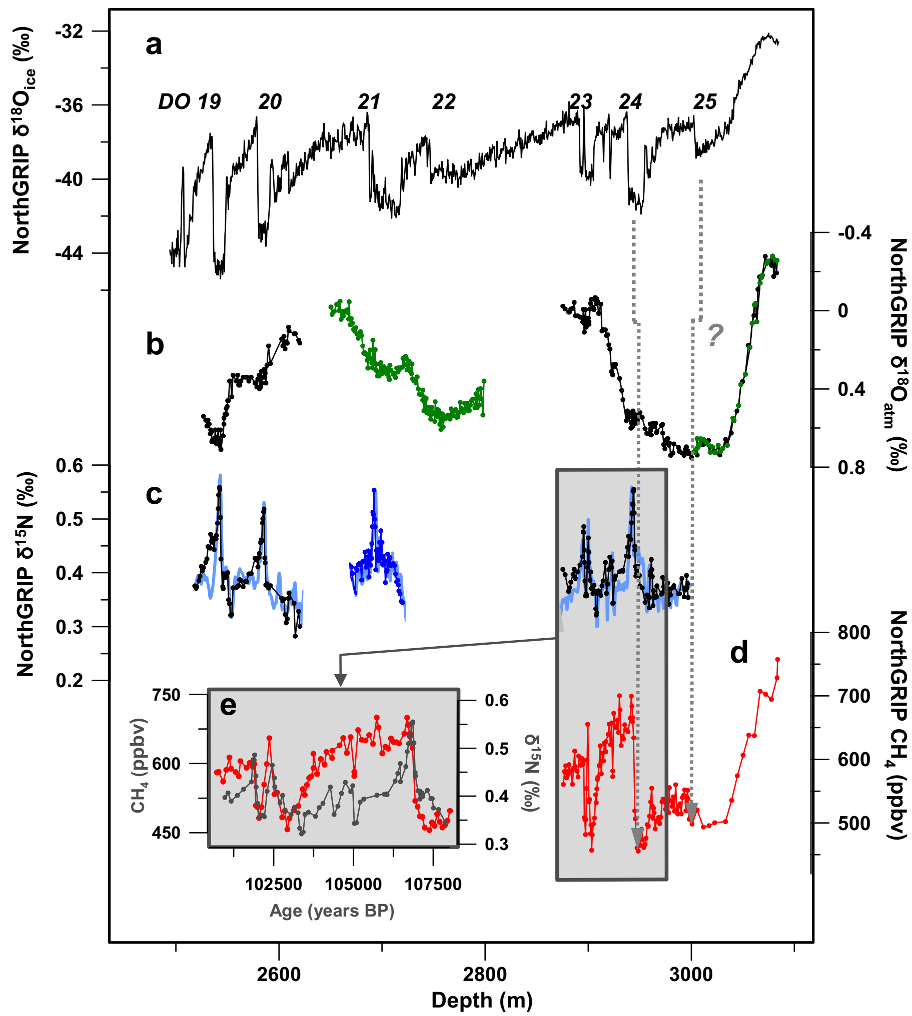

Fig. 1. NorthGRIP climate records plotted versus depth. (a) $\delta^{18}O_{ice}$, proxy of local temperature (NorthGRIP community members, 2004). (b) $\delta^{18}O_{atm}$ data; new measurements in green, data from Landais et al. (2006b, 2007) in black. Note that the measurements over the bottom part of the NorthGRIP ice core were performed through two different air extraction techniques and show a good agreement (Landais et al., 2010). (c) $\delta^{15}N$ measurements over DO events 19, 20, 21, 23 24 (in black: Landais et al., 2004; Landais et al., 2005, new data in dark blue), modelled $\delta^{15}N$ in light blue (Goujon et al., 2003). (d) CH_4 measurements. (e) Focus on the time interval corresponding to DO events 23 and 24. Within a few centimetres corresponding to less than 100 yrs, CH_4 and $\delta^{15}N$ increase in concert at the onsets of interstadials (Severinghaus et al., 1998; Severinghaus and Brook, 1999; Flückiger et al., 2004; Huber et al., 2006; Landais et al., 2006b; Grachev et al., 2007; Grachev et al., 2009). Assuming that this is the case for all DO events, $\delta^{15}N$ measurements on the NorthGRIP ice core can be used to identify the onset of DO events 19, 20 and 21 in the gas phase when CH_4 measurements are missing. The grey dotted arrow around DO event 24 relates the gas and ice records at the onset of DO event 24 interstadial; the grey dotted arrow around DO event 25 shows the ambiguous identification of this event in the gas phase through the CH_4 profile as the sequence of events seems opposite to the classical $\delta^{18}O_{ice}/CH_4$ relationship illustrated here with the DO event 24.

and chemical interferences of CO_2 and $\delta O_2/N_2$ are applied to improve measurement precision (details in Severinghaus et al., 2001; Landais et al., 2003). Note that comparison of $\delta^{18}O_{atm}$ measurements over DO event 25 with the two different air extraction techniques show an excellent agreement (Fig. 1b; Landais et al., 2010).

NorthGRIP raw $\delta^{18}O$ data must be corrected for gravitational and thermal isotopic fractionations located in the firn to obtain the $\delta^{18}O_{atm}$ profile following corrections procedure described in Landais et al. (2005, 2007). We only corrected EDML $\delta^{18}O$ values for gravitational fractionation since the Antarctic counterparts of DO events are neither rapid nor large enough to induce a detectable thermal anomaly (Caillon et al., 2001).

NorthGRIP measurements of $\delta^{18}O_{atm}$ have been corrected from the progressive gas loss during ice core storage (Landais et al., 2003; Severinghaus and Battle, 2006; Suwa and Bender, 2008) using $\delta O_2/N_2$ data, (for details see Landais et al., 2008). No correction for gas loss was applied on the EDML data set because values remain around $-12‰$ which is significantly more than the $-30‰$ observed for badly preserved ice (Landais et al., 2003). The final uncertainty (based on systematic duplicate measurements) is 0.06 ‰ for EDML $\delta^{18}O_{atm}$ measurements and 0.03 ‰ for NorthGRIP $\delta^{18}O_{atm}$. The final $\delta^{18}O_{atm}$ uncertainty is higher at EDML compared to NorthGRIP since (1) EDML $\delta^{15}N$ duplicate measurements (unpublished data) used for gravitational signal correction of $\delta^{18}O$ values show a stronger variability (0.02‰) than NorthGRIP $\delta^{15}N$ measurements (0.007‰) and (2) some NorthGRIP data (less than 5%) were discarded when associated reproducibility was too large.

Given the global character of the $\delta^{18}O_{atm}$, orbital-scale variations related to precession are common to the Vostok, EDML and NorthGRIP $\delta^{18}O_{atm}$ signals (Figs. 1 and 2; Bender et al., 1994; Petit et al., 1999; Shackleton, 2000; Dreyfus et al., 2007; Landais et al., 2010). Despite the absence of a timescale synchronisation, the good overlap between Vostok and EDML signals proves that the EDML ice core is undisturbed down to 2426 m depth and offers at least 149 kyr of continuous climatic history. Millennial-scale variability, already evidenced over MIS 4 (0.15‰ in 1000 yr) in the NorthGRIP ice core (Landais et al., 2007) and in Antarctica

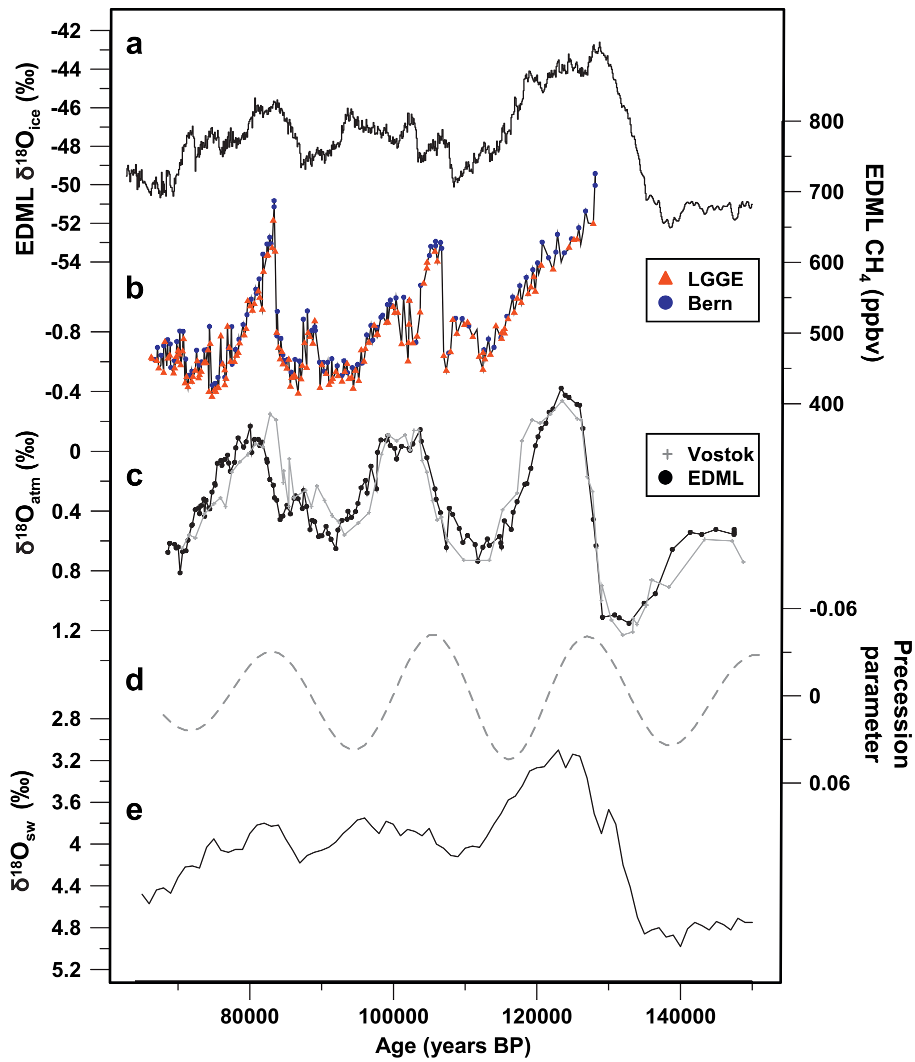

Fig. 2. (a) EDML $\delta^{18}O_{ice}$ (EPICA community members, 2006) on EDML1 timescale (Ruth et al., 2007). (b) CH_4 measurements (blue circles, University of Bern; red triangles, LGGE). (c) EDML $\delta^{18}O_{atm}$ measurements (black circles) superimposed on Vostok $\delta^{18}O_{atm}$ (grey crosses) measurements displayed on the original GT4 timescale (Petit et al., 1999). EDML gas measurements are displayed on the EDML gas timescale from Loulergue et al. (2007). (d) Precession parameter (Laskar et al., 2004). (e) $\delta^{18}O_{sw}$ (Lisiecki and Raymo, 2005).

(Severinghaus et al., 2009), is clearly evidenced over DO events 19 and 20 in the EDML $\delta^{18}O_{atm}$ signal. This millennial-scale variability superimposed to the long term evolution is also present over MIS 5, on DO events 21, 22, 23 and 24 for both NorthGRIP and EDML ice cores.

Fig. 1 presents a new data set of 59 duplicate measurements of $\delta^{15}N$ between 2680 m and 2710 m depth with a mean resolution of 1 m on the air trapped in the NorthGRIP ice. The $\delta^{15}N$ profile shows a rapid variation of 0.15 ‰ at 2694 m depth. This positive anomaly depicted in the $\delta^{15}N$ profile is the result of thermal fractionation associated with the onset of DO event 21 and is recorded 6–7 m deeper than the corresponding increase of $\delta^{18}O_{ice}$ as expected from firnification model (Fig. 1c; Goujon et al., 2003).

3. Construction of a common timescale between EDML and NorthGRIP ice cores

3.1. Construction of a common gas timescale based on CH_4 and $\delta^{15}N$ profiles

We first define tie points using only CH_4 and $\delta^{15}N$ measurements as stratigraphic markers (Fig. 3). The sharp CH_4 transitions enable us to clearly define tie points between the two cores, corresponding to the mid point of each CH_4 sharp increase and decrease. The strong DO event 24 can be precisely constrained through tie points at the onset and at the end of this event with an uncertainty of 290 yr (procedure for error estimate is detailed in the Appendix).

DO event 21 is also clearly seen in the EDML CH_4 record. In the absence of CH_4 measurements in the NorthGRIP ice core over this time period, we used the corresponding record of $\delta^{15}N$ of nitrogen in the gas trapped in the ice since CH_4 and $\delta^{15}N$ increase in concert within few decades at the beginning of DO events (Fig. 1e; Severinghaus et al., 1998; Severinghaus and Brook, 1999; Flückiger et al., 2004; Huber et al., 2006; Grachev et al., 2007, 2009). This leads to a precise tie point at the onset of DO event 21 associated with a mean uncertainty of 150 yr (Fig. 3; Table 1).

Correlations are less clear for the other DO events. The CH_4 signature of DO events 19 and 20 is not obvious in the EDML record as already observed in other Antarctic ice cores (Blunier and Brook, 2001). It is tempting to assign the 70–80 ppbv CH_4 variations observed at 71.0 and 74.7 kyr to the onset of DO events 19 and 20, respectively. However, CH_4 variations of the same magnitude are observed between 75.6 and 77.5 kyr in the absence of any significant climatic change, which questions this possible attribution.

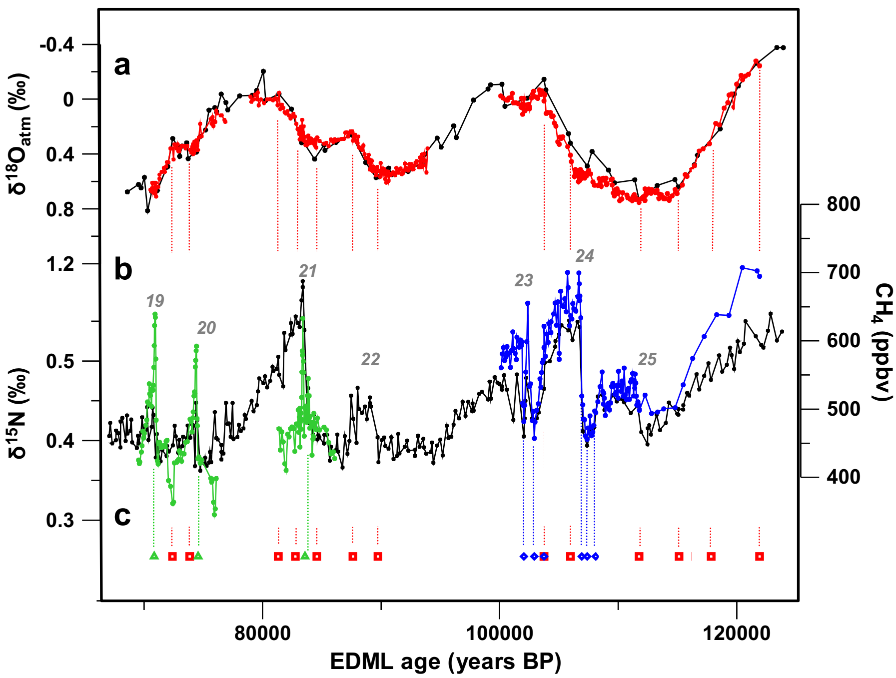

Fig. 3. EDML-NorthGRIP gas records synchronisation on the interval 70–123 kyr. (a) $\delta^{18}O_{atm}$ synchronisation between EDML (black dotted curve) and NorthGRIP (red dotted curve). (b) Synchronisation for the rapid temperature increases associated with DO events 19–25 (numbered in grey) through EDML CH_4 record (black dotted curve), NorthGRIP $\delta^{15}N$ record (green curve) and NorthGRIP CH_4 record (blue curve). (c) Gas age tie points corresponding to $\delta^{18}O_{atm}$ matching (red squares) and $\delta^{15}N/CH_4$ (green triangles) or CH_4 matching (blue diamonds). Those gas tie points are highlighted with vertical lines (same colour code).

The second problem is the onset of DO event 23. While the short precursor-type peak preceding the long warm phase of DO event 23 is clearly identified in the NorthGRIP record with a 150 ppbv change, the EDML record shows a double peak with a maximum amplitude of only 50 ppbv. The small amplitude difference of this short DO event in Antarctica could be partly explained by the existence of an interhemispheric gradient that attenuates CH_4 amplitude variations recorded in the Southern Hemisphere (Chappellaz et al., 1997; Dällenbach et al., 2000) and more likely by a stronger signal attenuation of fast atmospheric CH_4 variations recorded in the EDML ice core due to a lower accumulation rate compared to the NorthGRIP one. In fact, the CH_4 signature associated with DO events is attenuated during the enclosure processes in the ice (Spahni et al., 2003). Indeed, we estimate EDML CH_4 signal attenuation almost 3 times higher than at NorthGRIP by taking into account their respective surface characteristics using the approach of Spahni et al. (2003). Finally, considering the construction of the EDC and EDML gas timescales based on CH_4 records between 60 and 140 kyr (Loulergue, 2007), we reject the second peak as a precursor of the DO event 23. This would indeed imply a 1 kyr discrepancy between EDC and EDML gas age scales and, thus, contradict the firnification physics.

Table 1
Gas tie points used to correlate NorthGRIP and EDML records by minimizing the area between the NorthGRIP and EDML $\delta^{18}O_{atm}$ and CH_4 records and associated uncertainties. Note that synchronisation uncertainties are minimal for DO events 19, 20 and 21 thanks to the use of $\delta^{15}N$ (see Section 3.3.2).

	NG depth (m)	EDML depth (m)	EDML1 age (yrs BP)	Gas tracers	Uncertainties (yrs)
1	2544.0	1860	70853	*$\delta^{15}N/CH_4$ (DO 19)*	140
2	2552.5	1880.7	72401	*$\delta^{18}O_{atm}$*	*440*
3	2581.4	1902.2	73858	*$\delta^{18}O_{atm}$*	*260*
4	2586.4	1914.3	74563	*$\delta^{15}N/CH_4$ (DO 20)*	160
5	2667.1	1995.4	81325	*$\delta^{18}O_{atm}$*	*970*
6	2680.6	2011.6	82766	*$\delta^{18}O_{atm}$*	*180*
7	2694	2021.6	83578	*$\delta^{15}N/CH_4$ (DO 21)*	*150*
8	2704.4	2034.3	84577	*$\delta^{18}O_{atm}$*	*1220*
9	2721.9	2068.9	87627	*$\delta^{18}O_{atm}$*	*570*
10	2759.1	2091.5	89729	*$\delta^{18}O_{atm}$*	*1160*
11	2897.4	2198.0	102046	*CH_4*	*290*
12	2903.4	2204.5	102930	*CH_4 (DO 23)*	*290*
13	2911.7	2209.9	103747	*$CH_4/\delta^{18}O_{atm}$*	*290*
14	2932.6	2224.9	105971	*$\delta^{18}O_{atm}$*	*1000*
15	2945.2	2230.4	106935	*CH_4*	*290*
16	2948.5	2233.8	107382	*CH_4 (DO 24)*	*290*
17	2958.5	2239.0	108115	*CH_4*	*290*
18	3000.3	2259.9	111759	*$\delta^{18}O_{atm}$*	*1000*
19	3036.9	2285.5	115147	*$\delta^{18}O_{atm}$*	*880*
20	3053.3	2303.3	117860	*$\delta^{18}O_{atm}$*	*1110*
21	3073.1	2333.2	121929	*$\delta^{18}O_{atm}$*	*1970*

Third, it is tempting to identify the onset of DO event 25 as the 50 ppbv increase of CH_4 at 3000 m depth in the NorthGRIP ice core and match it with the similar CH_4 increase in the EDML record at 112.5 kyr. However, Fig. 1 shows that this increase in CH_4 occurs at a shallower depth than the $\delta^{18}O_{ice}$ increase corresponding to the onset of DO event 25 in the NorthGRIP ice core. This would mean that the CH_4 increase lags by several centuries the surface temperature change. Such asynchrony in the CH_4 and Greenland temperature challenges the observed synchronicity between the two signals for younger events and prevents us to use confidently the corresponding EDML CH_4 increase as a constraint for the onset of DO event 25.

Finally, matching EDML and NorthGRIP CH_4 records over the glacial inception is not possible. Indeed, the NorthGRIP ice core does not record the whole MIS 5e period (NorthGRIP community members, 2004) so that the peak CH_4 maximum cannot be identified on this ice core to provide a firm tie point. A direct matching of absolute CH_4 values between Antarctic and Greenland ice cores is not possible due to expected large changes in the interglacial interhemispheric gradient.

Summarizing, using only CH_4 and $\delta^{15}N$ profiles does not bring sufficient dating constraints to construct the EDML-NorthGRIP synchronisation (1) for the time interval 84–95 kyr which cover the Greenland rapid event, DO 22, and (2) prior to 108 kyr. Note, however, than when CH_4 data will become available over DO event 22 at NorthGRIP, it should enable to improve the synchronisation over the first aforementioned period.

3.2. Combining $\delta^{18}O_{atm}$ and CH_4 record to construct a common timescale

To complement tie points defined with CH_4 records, we identify control points (maxima, minima and mid-slopes) from $\delta^{18}O_{atm}$ records of NorthGRIP and EDML. In addition to the large amplitude variations linked with precession (Petit et al., 1999), we benefit from the superimposed millennial-scale variations which provide precise constraints over several DO events (Fig. 3; Table 1). As an example, over the 84–95 kyr period, the millennial-scale evolution of $\delta^{18}O_{atm}$ permits to define several tie points (Table 1): the long term decrease of $\delta^{18}O_{atm}$ accelerates strongly over the warm phase of DO event 22, followed by stable values during the stadial 21 and finally $\delta^{18}O_{atm}$ shows a strong decrease again during the warm phase of DO event 21.

During DO event 20, the long term $\delta^{18}O_{atm}$ increase is interrupted at 73.7 kyr when it remains constant until 72.4 kyr before a new long term decrease starts. The change in $\delta^{18}O_{atm}$ slope provides constraints over DO event 20 and confirms that the rapid 70–80 ppbv increase observed in the CH_4 record corresponds to the onset of the event. During the stadial preceding DO event 19, both NorthGRIP and EDML $\delta^{18}O_{atm}$ sharply increase and then decrease during the first part of the interstadial. This observation leads to the definition of an additional tie point, fully confirming the tie point suggested by the CH_4 records at 71.0 kyr.

Contrary to CH_4, $\delta^{18}O_{atm}$ is not affected by an interhemispheric gradient and this allows a synchronisation of the EDML and NorthGRIP $\delta^{18}O_{atm}$ records over the last glacial inception. Since the NorthGRIP ice core does not reach back to the $\delta^{18}O_{atm}$ minimum corresponding to MIS 5e, we match directly EDML and NorthGRIP $\delta^{18}O_{atm}$ absolute values along the glacial inception (Appendix). Supposing that a shift between the NorthGRIP and EDML $\delta^{18}O_{atm}$ profiles can exist after CH_4 record synchronisation as for the 105–115 kyr interval, it leads to larger uncertainties compared to time periods where CH_4 profiles are used or when $\delta^{18}O_{atm}$ extrema are clearly identified in the EDML and NorthGRIP records. This has been taken into account in the calculation of gas matching uncertainties (Table 1, Appendix) and in the determination of the north–south relationship over the first DO event 25 (Section 5; Table 2).

Finally, we derive a common gas chronology by using a linear interpolation of the depth levels over the 21 tie points linking the NorthGRIP gas depth to the EDML1 timescale (Table 1). This gas record synchronisation is associated with uncertainties determined by the resolution of the records and the visual choice of the tie points. For estimating the latter, ten different synchronisations have been generated using the Analyseries program (Paillard et al., 1996; see the Appendix for details).

Table 2
Quantification of the lag between the beginning of the Antarctic temperature increase over AIM events and the onset of corresponding DO events. The associated uncertainty is also shown in Fig. 5 (grey bars).

	Phasing	Uncertainty (years)
DO/AIM 20	1570	300
DO/AIM 21	3360	230
DO/AIM 22	760	610
DO/AIM 23	720	450
DO/AIM 24	1500	330
DO/AIM 25	500	1030

3.3. Transfer from the gas timescale to an ice timescale: Δage estimate

The ice age-gas age difference (Δage) has to be estimated for both NorthGRIP and EDML ice cores. Δage is calculated using firnification models (Herron and Langway, 1980; Barnola et al., 1991; Schwander et al., 1997; Arnaud et al., 2000; Goujon et al., 2003). These models have been empirically validated over a range of modern polar surface conditions (annual mean surface temperature between $-55.5\,°C$ and $-19\,°C$, accumulation rates between 2.1 cm w.e.yr^{-1} and 139.9 cm w.e.yr^{-1}).

Those firnification models can be tested using nitrogen isotopes measured in the air trapped in the ice since their fractionation only depend on physical processes in the firn. During period with no rapid temperature changes (<0.02 K yr^{-1}), $\delta^{15}N$ in the firn column is only affected by gravitational fractionation and brings information on the Diffusive Column Height (DCH) through the barometric equation (Craig et al., 1988; Sowers et al., 1992):

$$\delta^{15}\mathrm{N} = \Delta mgZ/\mathrm{R}T \quad (1)$$

where Δm is the mass difference between ^{15}N and ^{14}N (g mol^{-1}), g is the gravitation acceleration (ms^{-2}), Z, the DCH (m), R, the gas constant (JK^{-1} mol^{-1}) and T, the firn temperature (K). In Greenland, it has been shown that transient thermal gradients in the firn during the rapid surface temperature changes associated with DO events lead to additional variations of $\delta^{15}N$ trapped in the ice through thermal fractionation (Severinghaus et al., 1998).

The NorthGRIP Δage was calculated with the firnification and heat diffusion model from Goujon et al. (2003). When forced by the variations of temperature derived from $\delta^{18}O_{ice}$, the same firn densification model was shown to capture correctly the evolution of $\delta^{15}N$ variations (Fig. 1, Landais et al., 2008). This good agreement leads to a 10% uncertainty on Δage estimate (less than 100 yr) for the NorthGRIP ice core resulting from sensitivities studies of Arnaud et al. (2000) and Goujon et al. (2003).

The EDML Δage was calculated over the last 150 kyr by running the same firn densification model (Goujon et al., 2003; Loulergue et al., 2007). Classically, the model is forced by a temperature and accumulation rate scenario (hereafter noted Scenario 1 following Loulergue et al., 2007) deduced from $\delta^{18}O_{ice}$ following the equations prescribed in EPICA community members (Supplementary material, 2006). The EDML glacial-interglacial surface characteristics lie within the ranges of temperature and accumulation rate of present-day studied firns. However, as for other inland Antarctic sites, a strong mismatch between measured and modelled $\delta^{15}N$ was depicted at EDML over the deglaciation and the last glacial period (Caillon et al., 2003; Landais et al., 2006a; Capron et al., 2008). Such a mismatch casts doubts on the correct modelling of the DCH, thus on a correct estimate of Δage for the EDML ice core. We conclude that a 10% uncertainty on the EDML Δage estimate is not realistic. In the following, we will discuss three different approaches to constrain as precisely as possible the EDML Δage uncertainty, questioning temperature and accumulation scenarios as well as the firn model physics.

3.3.1. Estimate of EDML Δage uncertainties through independent markers in the gas and ice phases

Loulergue et al. (2007) evaluated their Δage estimate by using independent markers in the ice ($\delta^{18}O_{ice}$ and ^{10}Be) and in the gas (CH_4) at 40.4 kyr. (Yiou et al., 1997; Guillou et al., 2004; Raisbeck et al., 2007). They suggested that the modelled Δage at 40.4 kyr is too large by about 15%. To match the modelled and estimated Δage, Loulergue et al. (2007) ran the firn densification model with a new scenario proposing a larger accumulation rate during glacial period (defined as Scenario 4) compared to the initial accumulation estimate derived from $\delta^{18}O_{ice}$ (Scenario 1, EPICA community members, Supplementary material, 2006). If we extrapolate this method to the whole EDML timescale, we obtain a mean standard deviation between the two Δage estimates (inferred from Scenario 1 and Scenario 4, Fig. 5b) of less than 100 yr. Limits in the approach of Loulergue et al. (2007) concern several aspects: (1) they assume that the physics of firn densification in the model is correct for both sites, (2) they assume that the mismatch between EDML and EDC gas chronologies could only result from accumulation rate parameterisations. Although such approach was suitable to produce a roughly coherent gas chronology for both EPICA cores, it does not claim to provide the final answer on Δage estimates. In addition, although Δage estimates are relatively well constrained at the location of the ^{10}Be peak (through matching with the GICC05 timescale), their extrapolation to other depths of both sites, and in particular over MIS 4 and MIS 5, remains poorly constrained.

3.3.2. Estimate of EDML Δage uncertainties through variations of the forcing scenarios of the firnification model

The common chronology between EDML and NorthGRIP for MIS 2 and MIS 3 (EPICA community members, 2006) has a relative dating uncertainty of 400–800 yr mostly due to Δage estimate. This uncertainty has been estimated considering that the Δage uncertainty originates only from the uncertainty of the input parameters (Blunier et al., 2007). Using exactly the same approach, we show on Fig. 5b the range of possible EDML Δage, applying ± 25% on accumulation (equivalent to a ± 4 °C uncertainty on surface temperature) for both Scenario 1 and Scenario 4 from Loulergue et al. (2007). This estimate does not account for firnification model physics and may therefore underestimate the true Δage uncertainty.

3.3.3. Uncertainty on EDML Δage using $\delta^{15}N$ data

Using the firnification model, the simulated $\delta^{15}N$ is larger by 5–15% than the EDML measured values over MIS 4 and 5 (unpublished data). This clearly questions the validity of this model both for $\delta^{15}N$ and Δage. Here, we present an alternative method to estimate Δage by using $\delta^{15}N$ as a proxy of Lock-In-Depth (LID) (e.g. Sowers et al., 1992; Blunier et al., 2004; Bender et al., 2006). This approach enables us to discuss the phasing between the AIM and the onset of the rapid CH_4 increases (as a marker for the rapid warming of DO event in Greenland) on the EDML depth scale. The method is the following:

- First, we deduce the LID from the $\delta^{15}N$ data points over each interval (Fig. 4) using the barometric equation (Equation (1)) and considering only gravitational fractionation. Here we have chosen to display only $\delta^{15}N$ data corresponding to the onset of DO 21 and 24 (see caption of Fig. 4) for determinating the corresponding Δdepth.
- Second, the Δdepth for a depth z (depth difference between two synchronous events) is calculated through the following equation:

$$\Delta depth(z) = LID(z) \times 0.7 \times T(z) \quad (4)$$

Assuming that it is equivalent to the LID adjusted for compaction of the firn with a densification factor of 0.7 (Barnola et al., 1991) and a thinning factor noted T, which represents the ratio between the in-situ annual layer thickness on the initial annual layer thickness.

The error on Δdepth estimate arises from uncertainties on (i) the depth of the convective zone, the upper part of the firn where the well-mixed air has the same composition as the atmosphere and (ii) the thinning function. In equation (4), we have assumed that the convective zone is negligible by directly linking $\delta^{15}N$ to the LID. Large convective zones may exist in modern Antarctic sites with very low accumulation rates and temperatures (Caillon et al., 2001; Kawamura et al., 2006). The occurrence of past convective zones was inferred from the mismatch between the LID simulated by the firnification model and the systematically smaller LID deduced from $\delta^{15}N$ data (i.e. Caillon et al., 2001; Kawamura et al., 2006;

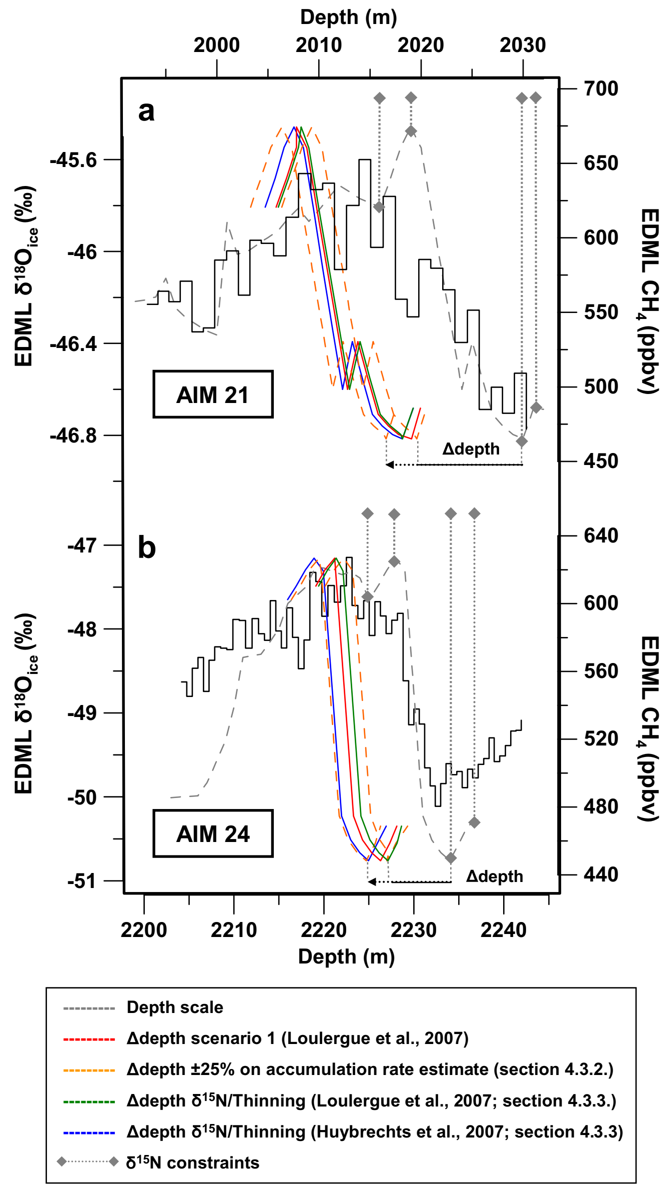

Fig. 4. Comparison of EDML $\delta^{18}O_{ice}$ (black)/CH_4 (original in grey) phasing obtained by the different methods of Section 3.3 over Greenland DO events 21 and 24 and their Antarctic counterparts, AIM 21 (a) and AIM 24 (b). For Δdepth calculations (Section 3.3.3), the location of $\delta^{15}N$ constraints (grey diamonds) have been taken at the onset and at the end of the rapid CH_4 increases. The corresponding shifted CH_4 curves are displayed in blue and green for Δdepth calculations using the thinning estimates from Huybrechts et al. (2007) and Loulergue et al. (2007) respectively. The red shifted CH_4 curve was obtained using the depth-age correspondence of Loulergue et al. (2007) calculated through firnification modelling (Goujon et al., 2003). The two dashed orange shifted CH_4 curves result from an uncertainty of 25% on accumulation rate used to calculate Δdepth with the firnification model (Section 3.3.2). The red, blue and green shifted CH_4 curves are systematically within the range depicted by the two orange shifted CH_4 curves so that the method depicted in Section 3.3.2 is shown to capture realistically the upper limit for Δdepth, hence Δage uncertainty range.

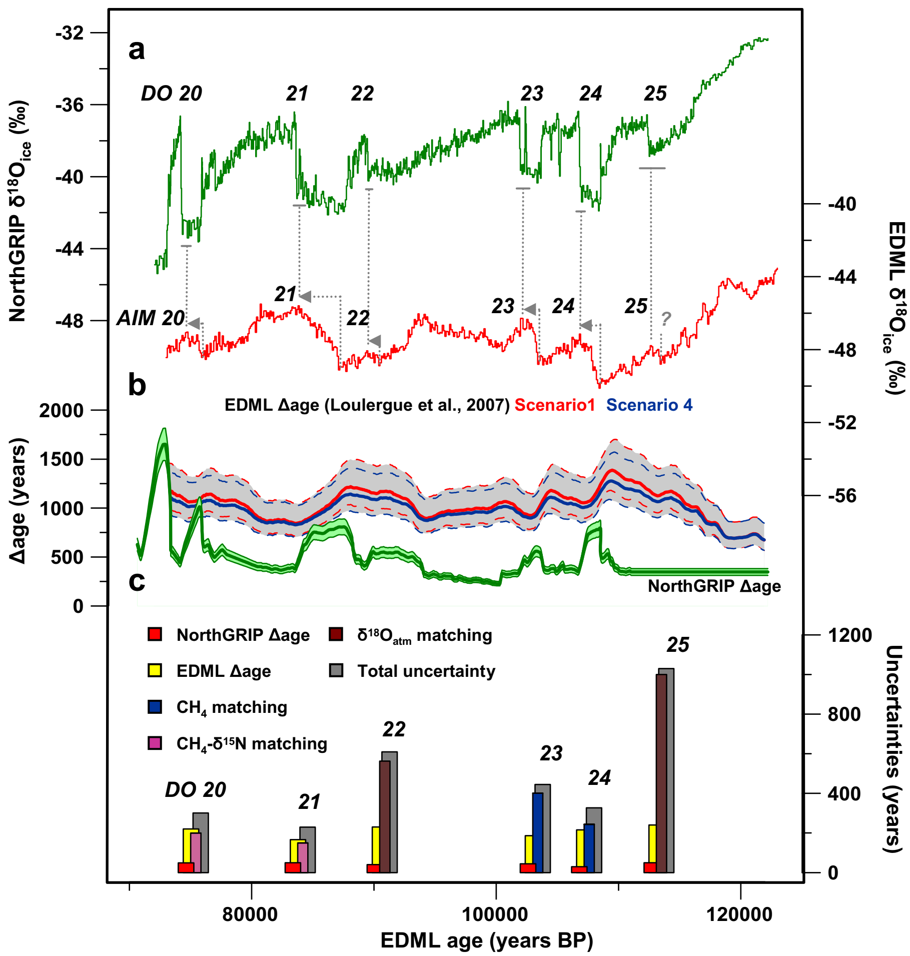

Fig. 5. Construction of a common ice timescale based on EDML1 for the NorthGRIP and EDML records. (a) NorthGRIP and EDML $\delta^{18}O_{ice}$ records. Grey arrows and grey vertical bars represent the phase relationship between onsets of AIM and DO events. (b) EDML (red curve) and NorthGRIP (green curve) Δage within their ranges of uncertainty (10% of Δage for NorthGRIP; for EDML – see Section 3.3.2). We extrapolate Scenario 1 and Scenario 4 used in Loulergue et al. (2007) to obtain Δage estimates for EDML. (c) Uncertainty of the synchronisation at the onset of the DO events: the red and yellow bars correspond respectively to the NorthGRIP and EDML Δage uncertainties. The gas synchronisation uncertainty depending on the stratigraphic tool used: CH_4 matching uncertainty, blue bar; $\delta^{18}O_{atm}$ matching uncertainty, brown bars and $\delta^{15}N/CH_4$ matching uncertainty, pink bars. The total uncertainty (grey bars) has been calculated by adding in quadrature all different uncertainties detailed above (Values are given Table 2).

Landais et al., 2006a, Dreyfus et al., 2010). The maximum depth of the convective zone corresponds to a situation where the model-data mismatch is compatible with a correct Δage simulation within the range of uncertainty of the input parameters, i.e. to the situation already depicted in Section 4.3.2. Here, by assuming no convective zone at EDML, we consider an extreme case and therefore a maximum uncertainty on the Δage determination.

We first evaluate the uncertainty on the thinning function by comparing the different available estimates. First, using a 2D glaciological model, Huybrechts et al. (2007) obtained a thinning function decreasing from 0.219 to 0.176 between 2016 m and 2236 m. With an inverse method combining glaciological models with tie points constraints between the EDML and the EDC ice cores, Lemieux-Dudon et al. (2010) find a thinning function decreasing from 0.196 to 0.146 between 2000 m and 2230 m. Finally, the thinning associated to the gas dating obtained by Loulergue et al. (2007) varies from 0.194 to 0.143 in the same depth interval. This comparison gives a mean uncertainty of 15% on the thinning function at each depth of MIS 5, similar to earlier estimates (Bender et al., 2006; Parrenin et al., 2007). The Δdepth method is applied on two depth intervals: (1) 2030 m to 2016 m including the rapid CH_4 increase at the onset of DO event 21 and the associated AIM (Fig. 4a) and (2) 2236 m to 2225 m including the rapid CH_4 increase at the onset of DO event 24 and the associated AIM (Fig. 4b). In each case, we used the $\delta^{15}N$ values at the depth levels corresponding respectively to the minimum and the maximum of the rapid CH_4 onset. Then, the corresponding Δdepth was deduced using the two extreme thinning values (Huybrechts et al., 2007; Loulergue et al., 2007). This Δdepth calculation permits to depict the sequence of events and especially the relative timing of rapid CH_4 increase and slow $\delta^{18}O_{ice}$ increase on the EDML depth scale (Fig. 4).

The last step is to compare the sequence of events obtained on a depth scale by using the $\delta^{15}N$ based method with the previous estimates (Sections 3.3.1 and 3.3.2). The age – depth correspondence for the EDML1 timescale is directly obtained from Ruth et al. (2007) and permits to directly visualize the phasing between the CH_4 increases (i.e. Greenland warming) and the $\delta^{18}O_{ice}$ increases (i.e. Antarctica warming) (Fig. 4). The comparison of the phasing between $\delta^{18}O_{ice}$ and CH_4 for the different scenarios shows that the uncertainty range obtained from Section 3.3.2 also encompasses the uncertainties of the $\delta^{15}N$ based method. Our Δdepth method provides an independent validation of our age scale and of the maximum dating uncertainties for EDML (Fig. 5b; Table 2).

4. Climatic implications

The EDML/NorthGRIP common ice timescale is displayed on Fig. 5. The total uncertainty (Fig. 5c) has been calculated by taking the quadratic average of uncertainties (i) of Δage for the two cores and (ii) linked with the different gas records tie points. The quantification of the exact phasing between the onsets of Antarctic warmings and rapid DO interstadials in Greenland has an accuracy of a few centuries except for the onset of DO event 25 where the total uncertainty remains higher than 1000 yr (See the Appendix).

From 80 to 123 kyr, this new synchronisation confirms the persistency of a north–south coupling with an Antarctic slow warming preceding Greenland abrupt warming by several centuries to several millennia (Table 2) and allows the extension of the Antarctic Isotope Maximum (AIM) nomenclature initially restricted to MIS 3 (EPICA community members, 2006) back to MIS 5 (Fig. 5a).

The Antarctic temperature increase associated with 5d/5c transition (106.8–108.4 kyr interval on EDML1 timescale) precedes the rapid temperature rise of DO event 24 by 1500 ± 330 yr. This robust result is well constrained by DO event 24 onset tie point inferred from the EDML and NorthGRIP CH_4 profiles. This phasing is consistent with the 2 kyr ($\pm$500 yr) obtained by Caillon et al. (2003) who used the rapid CH_4 increase recorded in the Vostok air as a proxies for rapid temperature change over Greenland and variations of $\delta^{15}N$ and $\delta^{40}Ar$ also measured in the Vostok air as proxy for local temperature change. The good agreement between the two methods shows that even if the processes driving changes in $\delta^{15}N$ and $\delta^{40}Ar$ are not fully understood in Antarctic ice cores (Landais et al., 2006a), these proxies can be used to detect temperature changes in the gas record as initially proposed by Caillon et al. (2003).

We also provide a description of the north–south coupling for the DO events 20 to 23. For each event, the onset of Antarctic warming leads Greenland abrupt warming, while the maximum of the warming is concomitant at both poles. For DO events 20, 21, 22 and 23, Antarctic temperature begins to increase respectively 1.7 ± 0.3 kyr, 3.4 ± 0.2 kyr, 0.8 ± 0.6 kyr and 0.9 ± 0.5 kyr before the abrupt temperature rise in Greenland. Compared to the pioneering results of Blunier and Brook (2001) over DO event 20 and 21 (respective lags of 1 kyr and 3.2 kyr), we confirm the asynchrony and reduce the uncertainty by more than a factor of 2. For the first time, we describe here the Antarctic counterparts AIM 22 and 25 of the small DO events 22 and 25, marked again by a lead of Antarctica with respect to Greenland for DO event 22. The north–south phasing over DO event 25 cannot however, be firmly determined because our matching uncertainty over the glacial inception is higher than 1 kyr.

MIS 5 lags (0.7–3 kyr) observed between Antarctic temperature increase and the onset of Greenland interstadials are consistent with those observed over MIS 3 (0.5–2 kyr) (EPICA community members, 2006). We confirm that peak warmth occurs in phase in Greenland and Antarctica all over MIS 5, an observation made already by Blunier and Brook (2001) back to 90 kyr. The sequence of millennial-scale climate variability between Greenland and Antarctica is therefore a pervasive characteristic from the first to the last DO event of the glacial period.

Our results thus contradict the possible existence of a critical threshold in ice sheet volume to induce climatic millennial-scale variability (McManus et al., 1999). Over MIS 3, the stadials before DO events 4, 8 and 12 are associated with major iceberg discharges respectively corresponding to Heinrich events 3, 4 and 5, respectively, whereas no such massive icebergs discharges are evidenced for MIS 5 (Heinrich, 1988; Bond et al., 1992). It challenges the straightforward link between ice volume and climate instabilities.

The bipolar seesaw mechanism is understood by changes in the heat and freshwater flux connected to the onset/collapse of the Atlantic Meridional Overturning Circulation (AMOC) and heat accumulation in the Southern Ocean (Stocker and Johnsen, 2003; Knutti et al., 2004). The evidence of a linear relationship between the warming amplitude of all AIM (inferred from the EDML $\delta^{18}O_{ice}$) and the concurrent stadial duration in Greenland over MIS 3 validated this theoretical concept (EPICA community members, 2006) but the study was restricted to MIS 3 rapid events. Our new EDML-NorthGRIP timescale enables to investigate this north–south dependency over MIS 5 (Fig. 6). We limit this study to AIM 21, 23, and 24 and their accompanying stadials from NorthGRIP $\delta^{18}O_{ice}$ considering that our timescale synchronisation is most robust over those rapid events and that a clear seesaw pattern is identified.

Within uncertainties, DO/AIM 23 and 24 lie on the regression line established for MIS 3 rapid events (Fig. 6; EPICA community members, 2006). They are comparable with the MIS 3 largest events, DO/AIM 4, 7, 8 and 12. This similar behaviour for events of MIS 3 and 5 shows that the Antarctic warming rate does not depend on climate background (i.e. different ice sheet volumes, greenhouse gas levels, temperature conditions and orbital configurations). This would support the use of one single characteristic timescale associated to the Southern Ocean heat reservoir to model the thermal bipolar seesaw (Stocker and Johnsen, 2003).

However, we note that AIM/DO 21 event significantly deviates from the linear regression line. The duration of the stadial prior to DO event 21 is exceptionally long (4 kyrs) and the Antarctic warming amplitude (4 °C) is the most important over the whole glacial period. This suggests that heat flow from the Southern Ocean is not constant during all AIM events and contradicts the hypothesis presented above of Stocker and Johnsen (2003) who assumed a Southern Ocean heat reservoir with only one characteristic timescale. Previous hypothesis also suggests that for long cessations of the AMOC, new temperature equilibrium in the Southern Ocean would be reached and the warming would become slower or eventually have to cease since the Southern Ocean cannot accumulate heat indefinitely (EPICA community members, 2006). However, within our age scale, the warming rate over AIM event 21

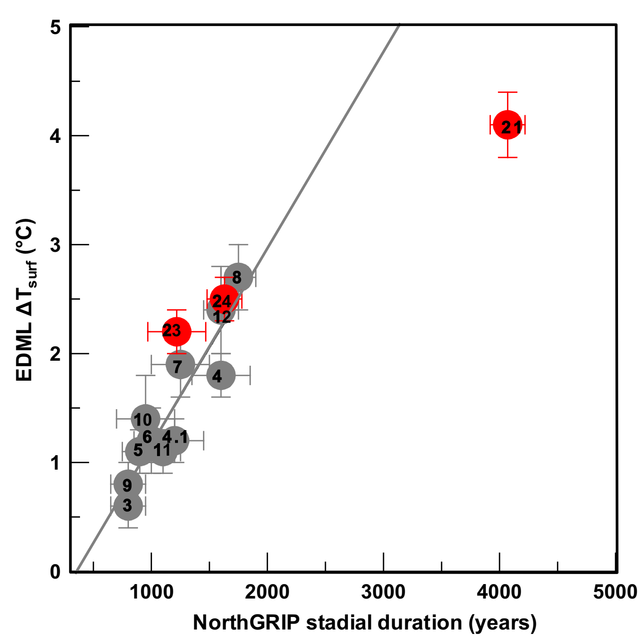

Fig. 6. Amplitudes of Antarctic warmings versus the duration of the concurrent stadial in Greenland for MIS 3 rapid events (grey points, EPICA community members, 2006) and for the DO/AIM events of MIS 5, 21, 23 and 24 (red points). The procedure for the determination of Antarctic warming amplitudes and Greenland stadial durations follows EPICA community members (2006). The labels corresponding to DO and AIM events are indicated. The grey line represents the linear fit established for all rapid events from MIS 3 (EPICA community members, 2006). Error bars show the uncertainties on the estimate of Antarctic warming amplitudes and Greenland stadial durations.

seems almost constant all over the stadial period, around two times slower than for AIM events 23 and 24 so that the rapid temperature increase in Greenland occurs when Antarctic is still warming and not on a temperature plateau.

Our new data confirm that the bipolar seesaw is a robust feature associated with the millennial-scale climatic variability of the full duration of the last glacial period. They reveal that Antarctic warming rate and thus the latitudinal heat transport can vary between events, limiting the use of conceptual models to quantitatively describe this phenomenon. More complex models should be used and take into account parameters such as several characteristic timescales, the heat reservoir size or different deep-water formation rates.

5. Summary and perspectives

- For the first time, we have combined the millennial-scale variability of both CH_4 and $\delta^{18}O_{atm}$ records measured at high resolution on two ice cores (EDML and NorthGRIP) to produce a common gas timescale between Greenland and Antarctica with quantified and minimal associated uncertainties over the 70–123 kyr period.
- The accuracy of the ice record synchronisation mainly depends on the Δage calculation. With a new model-independent method based on $\delta^{15}N$ measurements, we have reduced the Δage uncertainty at EDML to a few hundreds of years, i.e. considerably less than in central Antarctic ice cores (a thousand years).
- We have presented the first continuous north–south synchronisation for the 70–123 kyr time interval and thus extended the study of the north–south climatic asynchrony of Blunier and Brook (2001) and EPICA community members (2006) to the entire sequence of MIS 5 DO events. The onset of millennial-scale warmings in Antarctica has been shown to precede the onset of warming in Greenland by 0.7–3 kyr in agreement with the leads observed over MIS 3.
- While the bipolar seesaw is a clear feature operational from the beginning of the glacial period, the relationship between Antarctic warming amplitudes and the duration of the Greenland concurrent stadials over MIS 5 differs for DO event 21 and other DO events. This suggests variability in the oceanic circulation overturning rate between the rapid events independently of the climate background state. This deserves to be further explored with sensitivity tests run with coupled Ocean-Atmosphere models.
- Isotopic data from East Antarctic sites (Dome C, Jouzel et al., 2007; Dome F, Kawamura et al., 2007) suggest a "shoulder" in δD or $\delta^{18}O_{ice}$ over the glacial inception as a possible counterpart to DO event 25 but the lack of a synchronisation with a Greenland record prevents a precise description of the climatic event sequence. Our synchronisation approach on EDML and NorthGRIP failed to provide a precise synchronisation of EDML and NorthGRIP around DO event 25 and its potential Antarctic counterpart. A definitive status on the set up of this interhemispheric coupling will require (i) high resolution measurements of CH_4 on the NorthGRIP record, (ii) a reconstruction of the local temperature signal at EDML to assess if the event recorded in the $\delta^{18}O_{ice}$ is a true climatic event considering changes in moisture origin (Stenni et al., 2010) and of surface elevation variations and ice origin changes at the EDML drilling site (EPICA community members, 2006; Huybrechts et al., 2007).
- The future NEEM deep drilling is expected to deliver a Greenland ice core older than MIS 5.4. This ice core would allow expanding the comparison of Greenland-Antarctic climate over the whole last interglacial period and Termination II.

Acknowledgments

We appreciate helpful discussions with J. Jouzel. We thank F. Parrenin for dating issue discussions and B. Minster, A. Bouygues, and G. Teste for their help on gas measurements. We are grateful to Hubertus Fischer and two anonymous reviewers who helped to improve the manuscript. This work was supported by ANR PICC and ANR NEEM and is a contribution to the European Project for Ice Coring in Antarctica (EPICA), a joint European Science Foundation/European Commission scientific programme, funded by the EU (EPICA-MIS) and by national contributions from Belgium, Denmark, France, Germany, Italy, the Netherlands, Norway, Sweden, Switzerland and the United Kingdom. The main logistic was provided by IPEV and PNRA (at Dome C) and AWI (at Dronning Maud Land). This is EPICA publication no. 231. This work is a contribution to the North Greenland Ice Core Project (NGRIP) directed and organized by the Department of Geophysics at the Niels Bohr Institute for Astronomy, Physics and Geophysics, University of Copenhagen. It is supported by funding agencies in Denmark (SNF), Belgium (FNRS-CFB), France (IPEV and INSU/CNRS), Germany (AWI), Iceland (RannIs), Japan (MEXT), Sweden (SPRS), Switzerland (SNF) and the USA (NSF, Office of Polar Programs). This is LSCE contribution number 4008.

Appendix. Error estimate linked to our gas records synchronisation

Ice cores synchronisation through global gas records is affected by several sources of uncertainties: (i) the gas records matching and (ii) the uncertainty of Δage for the two ice cores. Section 3.3 is dedicated to point (ii). For point (i), the uncertainty depends on the resolution of the records and on visual matching biases as explained below.

1. EDML/NorthGRIP CH_4 matching

Sharp variations of CH_4 over DO events 23 and 24 recorded both in the EDML and NorthGRIP ice cores allow the identification of precise mid-slope tie points. The gas synchronisation uncertainty is, therefore, only dependant on the resolution of the records. The uncertainty is calculated as the square root of the sum of squares of the EDML and NorthGRIP time resolution (Table 1).

2. NorthGRIP $\delta^{15}N$/EDML CH_4 matching

Within sampling resolution, CH_4 and $\delta^{15}N$ have been shown to increase in concert during rapid temperature change (Severinghaus et al., 1998, Severinghaus and Brook, 1999, Huber et al., 2006, Flückiger et al., 2004, Grachev et al., 2007, 2009). Thus, as for CH_4 matching, the error estimate results only from the square root of the sum of squares of the $\delta^{15}N$ and CH_4 record time resolution. We obtain a mean $\delta^{15}N/CH_4$ matching uncertainty of 150 yrs at the onset of DO events 19, 20 and 21, mostly due to the EDML CH_4 record resolution (Table 1).

3. EDML/NorthGRIP $\delta^{18}O_{atm}$ matching

A matching via CH_4 records cannot be done:

(i) For the 84–102 kyr period covering the DO event 22, since no CH_4 measurements have yet been performed in the NorthGRIP ice core;
(ii) Over DO event 25: the non-synchronicity between abrupt temperature increase and rapid CH_4 variations (described in Section 3.1) prevents us from using confidently this method;

(iii) Before 110 kyr: the NorthGRIP ice core does not capture the CH_4 maximum corresponding to MIS 5e that is necessary to define a mid-slope tie point over the glacial inception. The interhemispheric gradient affecting CH_4 concentration precludes any absolute CH_4 levels matching.

Thus, we used $\delta^{18}O_{atm}$ profile synchronisation over those time periods. Millennial-scale variability superimposed on orbital-scale $\delta^{18}O_{atm}$ variations over DO event 22 permits to define additional markers. In general, tie points are defined at slope breaks. One exception is the bottom part (below 3000 m depth) of the NorthGRIP ice core since the corresponding $\delta^{18}O_{atm}$ record does not display a clear minimum at 124 kyr. The only possibility to extend the synchronisation between 110 and 124 kyr is thus to match $\delta^{18}O_{atm}$ absolute values which are not affecting by pole-to-pole gradient.

The relatively slow temporal variations of $\delta^{18}O_{atm}$ record and the low resolution associated with the EDML record make it difficult to define a systematic procedure for tie point identification. Sensitivity tests were conducted and ten different visual matchings were performed using the Analyseries program (Paillard et al., 1996). Combined with the limitations caused by the data resolution, this leads to uncertainties on $\delta^{18}O_{atm}$ tie points of up to 1200 yrs.

Fig. A1 displays the match of the EDML and NorthGRIP $\delta^{18}O_{atm}$ records and its uncertainty range. This permits to visualize the result of our subjective visual matching. Over DO 19 and 20, the uncertainty is rather small because (i) we have confirmation of our $\delta^{18}O_{atm}$ visual matching by two CH_4 tie points and (ii) the resolution of the EDML $\delta^{18}O_{atm}$ record is relatively high (400 yrs). Over DO 22 (90 kyrs), only $\delta^{18}O_{atm}$ matching has been used and the resulting uncertainty is about 500–1000 yrs.

Over DO events 23 and 24, where many CH_4 tie points are available, we observe a surprising shift between NorthGRIP and EDML $\delta^{18}O_{atm}$ records: NorthGRIP $\delta^{18}O_{atm}$ values are heavier than the EDML ones by 0.1 ‰. This shift is neither observed over DO events 19 to 20 nor over DO 21 where $\delta^{18}O_{atm}$ was also combined to CH_4 for the gas synchronisation. Such a shift is probably due to a problem of storage effect on the NorthGRIP $\delta^{18}O_{atm}$ values since $\delta^{18}O_{atm}$ record covering DO events 23 and 24 were performed in spring 2004 on ice stored at temperature between −15 °C and −20 °C while $\delta^{18}O_{atm}$ NorthGRIP records covering DO events 19–20 and DO event 21 were respectively measured in Spring 2002 and Summer 2007, respectively, on ice stored below −20 °C.

We now discuss the uncertainty associated with the dating of the bottom part of the NorthGRIP ice core through $\delta^{18}O_{atm}$ only. First, the blue curve stands for the oldest dating of the NorthGRIP bottom part. Indeed, shifting the blue curve to the right means matching an increase of $\delta^{18}O_{atm}$ in the EDML ice core (before 124 kyr) and a decrease of $\delta^{18}O_{atm}$ in the NorthGRIP ice core which is impossible given the global character of this tracer. We thus consider that the shift between the red curve and the blue curve represents the maximum uncertainty on the dating and the green curve has been built as the symmetric of the blue curve with respect to the black one.

Since a shift of 0.1 ‰ in $\delta^{18}O_{atm}$ has been observed between the NorthGRIP and EDML record over the period encompassing DO events 23 and 24, it can be argued that a similar problem can affect our dating of the bottom part of the NorthGRIP ice core. However, we do not expect any gas storage effect on the NorthGRIP samples over this depth range: the first set of ice samples (low resolution) has been measured just after ice drilling hence with no storage effect detected in the O_2/N_2 ratio; the second set of samples was stored for 4 years at −25 °C and did not show strong storage effect ($\delta O_2/N_2$ around −10 ‰). Moreover, we note that we observe a $\delta^{18}O_{atm}$ 0.2‰ shift between the green (or the blue) curve and the red curve so that even if such storage effect has occurred, it is included in our error bar.

Note that our age markers give a uniform evolution of age as a function of depth with less than 10% deviation from the slope deduced from the age/depth relationship of the NorthGRIP glaciological timescale (NorthGRIP c.m., 2004). Thus, our timescale built from gas age markers seems also coherent with ice flow conditions at the NorthGRIP site. The major difference is obtained at the bottom of the NorthGRIP ice core for which the glaciological timescale is not strongly constrained because of the basal melting.

Finally to estimate the total synchronisation uncertainty we added the uncertainties linked with the Δage determination for each ice core. The mean uncertainty is less than 400 yrs for DO events 20 to 24 but remains higher than 1000 yrs after 110 kyr (Fig. 5; Table 2).

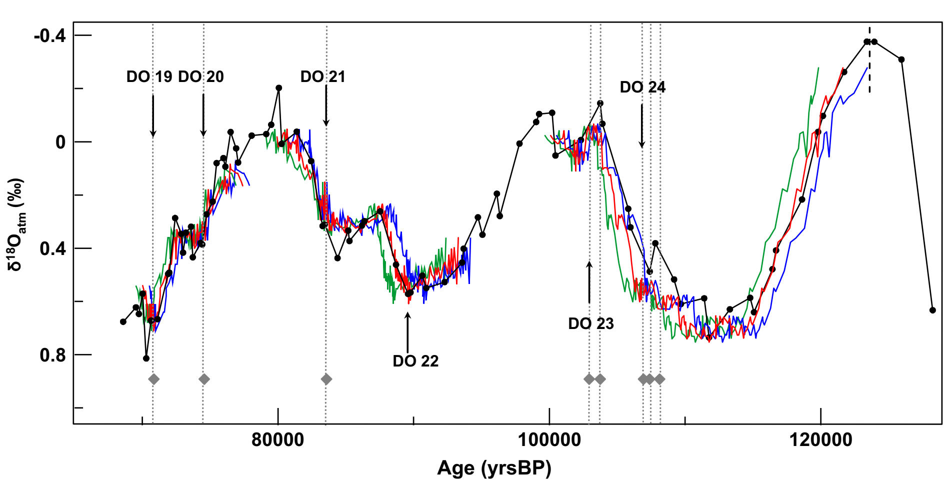

Fig. A1. EDML (black curve) and NorthGRIP (red curve) $\delta^{18}O_{atm}$ synchronisation on the EDML gas timescale (Loulergue et al., 2007). Green and blue $\delta^{18}O_{atm}$ profiles are extreme NorthGRIP $\delta^{18}O_{atm}$ curves obtained with shifts of the constructed timescale by taking into account the gas synchronisation uncertainties (Table 1). Grey diamonds signal CH_4- and NorthGRIP $\delta^{15}N$/EDML CH_4- tie points. The dashed line at 125 kyr highlights the EDML $\delta^{18}O_{atm}$ minimum corresponding to MIS 5e period not recorded in the NorthGRIP ice core. Black arrows mark the onset of DO events 19, 20, 21, 22, 23 and 24.

References

Arnaud, L., Barnola, J.M., Duval, P., 2000. Physical modeling of the densification of snow/firn and ice in the upper part of polar ice sheets. In: Hondoh, T. (Ed.), Physics of Ice Core Records, pp. 285–305. Sapporo.

Barnola, J.M., Pimienta, P., Raynaud, D., Korotkevich, Y.S., 1991. CO_2-Climate relationship as deduced from the Vostok ice core – a reexamination based on new measurements and on a reevaluation of the air dating. Tellus Series B-Chemical and Physical Meteorology 43, 83–90.

Bender, M., Sowers, T., Dickson, M.L., Orchardo, J., Grootes, P., Mayewski, P.A., Meese, D.A., 1994. Climate correlations between Greenland and Antarctica during the past 100,000 years. Nature 372, 663–666.

Bender, M., Malaizé, B., Orchardo, J., Sowers, T., Jouzel, J., 1999. High precision correlations of Greenland and Antarctic ice core records over the last 100 kyrs. Mechanisms of Global Climate Change at Millenial Time scales, Geophysical Monograph 112, 149–164.

Bender, M., Floch, G., Chappellaz, J., Suwa, M., Barnola, J.M., Blunier, T., Dreyfus, G., Jouzel, J., Parrenin, F., 2006. Gas age-ice age differences and the chronology of the Vostok ice core, 0–100 ka. Journal of Geophysical Research 111. doi:10.1029/2005JD006488.

Bintanja, R., van de Wal, R.S.W., Oerlemans, J., 2005. Modelled atmospheric temperatures and global sea levels over the past million years. Nature 437, 125–128.

Blunier, T., Chappellaz, J., Schwander, J., Dällenbach, A., Stauffer, B., Stocker, T.F., Raynaud, D., Jouzel, J., Clausen, H.B., Hammer, C.U., Johnsen, S.J., 1998. Asynchrony of Antarctic and Greenland climate change during the last glacial period. Nature 394, 739–743.

Blunier, T., Brook, E.J., 2001. Timing of millennial-scale climate change in Antarctica and Greenland during the last glacial period. Science 291, 109–112.

Blunier, T., Schwander, J., Chappellaz, J., Parrenin, F., Barnola, J.M., 2004. What was the surface temperature in central Antarctica during the last glacial maximum? Earth and Planetary Science Letters 218, 379–388.

Blunier, T., Spahni, R., Barnola, J.M., Chappellaz, J., Loulergue, L., Schwander, J., 2007. Synchronization of ice core records via atmospheric gases. Climate of the Past 3, 365–381.

Bond, G., Heinrich, H., Huon, H., Broecker, W.S., Labeyrie, L., Andrews, J., McManus, J., Clasen, S., Tedesco, K., Jantschik, R., Simet, C., 1992. Evidence for massive discharges of icebergs into the glacial Northern Atlantic. Nature 360, 245–249.

Caillon, N., Severinghaus, J.P., Jouzel, J., Barnola, J.M., Kang, J., Lipenkov, V.Y., 2001. Timing of atmospheric CO_2 and Antarctic temperature changes across termination III. Science 299, 1728–1731.

Caillon, N., Jouzel, J., Severinghaus, J.P., Chappellaz, J., Blunier, T., 2003. A novel method to study the phase relationship between Antarctic and Greenland climates. Geophysical Research Letters 30, 1899.

Capron, E., Landais, A., Masson-Delmotte, V., Leuenberger, M., Barnola, J.M., Oerter, H., 2008. Isotopic Composition of the Air Trapped in the EDML Ice Core ($\delta^{15}N$, $\delta^{18}Oatm$, $\delta^{40}Ar$, $\delta O_2/N_2$) Over the Last 140 kyrs. EGU, Vienna (Austria).

Chappellaz, J., Blunier, T., Kints, S., Dällenbach, A., Barnola, J.M., Schwander, J., Raynaud, D., Stauffer, B., 1997. Changes in the atmospheric CH_4 gradient between Greenland and Antarctica during the Holocene. Journal of Geophysical Research 102, 15987–15997.

Chappellaz, J., Blunier, T., Raynaud, D., Barnola, J.M., Schwander, J., Stauffer, B., 1993. Synchronous Changes in Atmospheric CH_4 and Greenland Climate between 40 kyr and 8 kyr BP. Nature 366, 443–445.

Craig, H., Horibe, Y., Sowers, T., 1988. Gravitational separation of gases and isotopes in polar ice caps. Science 242, 1675–1678.

Dällenbach, A., Blunier, T., Flückiger, J., Stauffer, B., Chappellaz, J., Raynaud, D., 2000. Changes in the atmospheric CH_4 gradient between Greenland and Antarctica during the Last Glacial and the transition to the Holocene. Geophysical Research Letters 27, 1005–1008.

Dansgaard, W., Johnsen, S., Clausen, H.B., Dahl-Jensen, D., Gundestrup, N., Hammer, C.U., Oeschger, H., 1984. North Atlantic climatic oscillations revealed by deep Greenland ice cores. In: Hansen, J.E., Takahashi, T. (Eds.), Climate Processes and Climate Sensitivity. AGU, Washington, D.C., pp. 288–298. 29.

Dreyfus, D., Jouzel, J., Bender, M.L., Landais, A., Masson-Delmotte, V., Leuenberger, M., 2010. Firn processes and $\delta^{15}N$: potential for a gas-phase climate proxy. Quaternary Science Reviews 29, 28–42.

Dreyfus, G.B., Parrenin, F., Lemieux-Dudon, B., Durand, G., Masson-Delmotte, V., Jouzel, J., Barnola, J.M., Panno, L., Spahni, R., Tisserand, A., Siegenthaler, U., Leuenberger, M., 2007. Anomalous flow below 2700 m in the EPICA Dome C ice core detected using $\delta^{18}O$ of atmospheric oxygen measurements. Climate of the Past 3, 341–353.

EPICA community members, 2006. One-to-one coupling of glacial climate variability in Greenland and Antarctica. Nature 444, 195–198.

Flückiger, J., Blunier, T., Stauffer, B., Chappellaz, M., Spahni, R., Kawamura, K., Schwander, J., Stocker, T.F., Dahl-Jensen, D., 2004. N_2O and CH_4 variations during the last glacial epoch: insight into global processes. Global Biogeochemical Cycles 18. doi:10.1029/2003GB002122.

Goujon, C., Barnola, J.M., Ritz, C., 2003. Modeling the densification of polar firn including heat diffusion: application to close-off characteristics and gas isotopic fractionation for Antarctica and Greenland sites. Journal of Geophysical Research 108 (D24), 4792.

Grachev, A., Brook, E.J., Severinghaus, J.P., 2007. Abrupt changes in atmospheric methane at the MIS 5b-5a transition. Geophysical Research Letters 34. doi:10.1029/2007GL029799.

Grachev, A.M., Brook, E.J., Severinghaus, J.P., Pisias, N.G., 2009. Relative timing and variability of atmospheric methane and GISP2 oxygen isotopes between 68 and 86 ka. Global Biogeochemical Cycles 23. doi:10.1029/2008GB003330.

Guillou, H., Singer, B.S., Laj, C., Scaillet, S., Jicha, B.R., 2004. On the age of the Laschamp geomagnetic excursion. Earth and Planetary Science Letters, 331–343.

Heinrich, H., 1988. Origin and consequences of cyclic ice-rafting in the northeast Atlantic Ocean during the past 130,000 years. Quaternary Research 29, 142–152.

Herron, M., Langway, C., 1980. Firn densification: an empirical model. Journal of Glaciology 25, 373–385.

Huber, C., Leuenberger, M., Spahni, R., Flückiger, J., Schwander, J., Stocker, T.F., Johnsen, S., Landais, A., Jouzel, J., 2006. Isotope calibrated Greenland temperature record over Marine Isotope Stage 3 and its relation to CH_4. Earth and Planetary Science Letters 243, 504–519.

Huybrechts, P., Rybak, O., Pattyn, F., Ruth, U., Steinhage, D., 2007. Ice thinning, upstream advection, and non climatic biases for the upper 89% of the EDML ice core from a nested model of the Antarctic ice sheet. Climate of the Past 3, 577–589.

Jouzel, J., Lorius, C., Johnsen, S., Grootes, P., 1994. Climate instabilities – Greenland and Antarctic records. C.R. Geosciences 319, 65–77.

Jouzel, J., Masson-Delmotte, V., Cattani, O., Dreyfus, G., Falourd, S., Hoffmann, G., Minster, B., Nouet, J., Barnola, J.M., Fisher, H., Gallet, J.C., Johnsen, S., Leuenberger, M., Loulergue, L., Luethi, D., Oerter, H., Parrenin, F., Raisbeck, G., Raynaud, D., Schilt, A., Schwander, J., Selmo, J., Souchez, R., Spahni, R., Stauffer, B., Steffensen, J.P., Stenni, B., Stocker, T.F., Tison, J.L., Werner, M., Wolff, E.W., 2007. Orbital and millenial Antarctic climate variability over the past 800,000 years. Science 317, 793–796.

Kawamura, K., Severinghaus, J.P., Ishidoya, S., Sugawara, S., Hashida, G., Motoyama, H., Fujii, Y., Aoki, S., Nakazawa, T., 2006. Convective mixing of air in firn at four polar sites. Earth and Planetary Science Letters 244, 672–682.

Kawamura, K., Parrenin, F., Lisiecki, L., Uemura, R., Vimeux, F., Severinghaus, J.P., Hutterli, M.A., Nakazawa, T., Aoki, S., Jouzel, J., Raymo, M.E., Matsumoto, K., Nakata, H., Motoyama, H., Fujita, S., Goto-Azuma, K., Fujii, K., Watanabe, O., 2007. Northern hemisphere forcing of climatic cyles over the past 360,000 years implied by accurately dated Antarctic ice cores. Nature 448, 912–916.

Knutti, R., Flückiger, J., Stocker, T.F., Timmermann, A., 2004. Strong hemispheric coupling of glacial climate through freshwater discharge and ocean circulation. Nature 430, 851–856.

Landais, A., Caillon, N., Severinghaus, J., Jouzel, J., Masson-Delmotte, V., 2003. Analyses isotopiques à haute précision de l'air piégé dans les glaces polaires pour la quantification des variations rapides de température: méthodes et limites. Notes des activités instrumentales de l'IPSL note n°39.

Landais, A., Barnola, J.M., Masson-Delmotte, V., Jouzel, J., Chappellaz, J., Caillon, N., Huber, C., Leuenberger, M., Johnsen, S.J., 2004. A continuous record of temperature evolution over a sequence of Dansgaard-Oeschger events during Marine Isotopic Stage 4 (76 to 62 kyr BP). Geophysical Research Letters 31. doi:10.1029/2004GL021193.

Landais, A., Barnola, J.M., Kawamura, K., Caillon, N., Delmotte, M., Van Ommen, T., Dreyfus, G., Jouzel, J., Masson-Delmotte, V., Minster, B., Freitag, J., Leuenberger, M., Schwander, J., Huber, C., Etheridge, D., Morgan, V., 2006a. Firn-air $\delta^{15}N$ in modern polar sites and glacial-interglacial ice: a model-data mismatch during glacial periods in Antarctica? Quaternary Science Reviews 25, 49–62.

Landais, A., Jouzel, J., Masson-Delmotte, V., Caillon, N., 2005. Large temperature variations over rapid climatic events in Greenland: a method based on air isotopic measurements. Comptes Rendus Geoscience 337, 947–956.

Landais, A., Masson-Delmotte, V., Jouzel, J., Raynaud, D., Johnsen, S., Huber, C., Leuenberger, M., Schwander, J., Minster, B., 2006b. The glacial inception as recorded in the NorthGRIP Greenland ice core: timing, structure and associated abrupt temperature changes. Climate Dynamics 26, 273–284.

Landais, A., Masson-Delmotte, V., Combourieu Nebout, N.C., Jouzel, J., Blunier, T., Leuenberger, M., Dahl-Jensen, D., Johnsen, S., 2007. Millenial scale variations of the isotopic composition of atmospheric oxygen over Marine Isotopic Stage 4. Earth and Planetary Science Letters 258, 101–113.

Landais, A., Sanchez Goñi, M.F., Masson-Delmotte, V., Jouzel, J., Barnola, J.M., Chappellaz, J., Leuenberger, M., Blunier, T., Dahl-Jensen, D., Johnsen, S.J., 2008. Continuous Air Isotopic Measurements Over MIS 4 and 5 in the NorthGRIP Ice Core (Greenland): New Constraints on the Sequences of Dansgaard–Oeschger (DO) Events and Links with Environmental Changes. EGU, Vienna (Austria).

Landais, A., Dreyfus, D., Capron, E., Sanchez-Goni, M.F., Desprat, S., Jouzel, J., Hoffmann, G., Johnsen, S., 2010. What drive orbital- and millennial-scale variations of the $\delta^{18}O$ of atmospheric oxygen? Quaternary Science Reviews 29, 235–246.

Laskar, J., Robutel, P., Joutel, F., Gastineau, M., Correia, A.C.M., Levrard, B., 2004. A long-term numerical solution for the insolation quantities of the Earth. A&A 428, 261–285.

Lemieux-Dudon, B., Parrenin, F., Waelbroeck, C., Barnola, J.M., 2010. Consistent dating for Antarctica and Greenland ice cores. Quaternary Science Reviews 29, 8–20.

Leuenberger, M.C., 1997. Modeling the signal transfer of seawater $\delta^{18}O$ to the $\delta^{18}O$ of atmospheric oxygen using a diagnostic box model for the terrestrial and marine biosphere. Journal of Geophysical Research 102, 26841–26850.

Lisiecki, L.E., Raymo, M.E., 2005. A Pliocene-Pleistocene stack of 57 globally distributed benthic delta O-18 records. Paleoceanography 20, PA1003. doi:10.1029/2004PA001071.

Loulergue, L., 2007. Contraintes chronologiques et biogéochimiques grâce au méthane dans la glace naturelle: une application aux forages du projet EPICA. phD thesis, Université Joseph Fourrier, pp. 257.

Loulergue, L., Parrenin, F., Barnola, J.M., Spahni, R., Schilt, A., Raisbeck, G., Chappellaz, J., 2007. New constraints on the gas-ice age difference along the EPICA ice cores, 0–50 kyr. Climate of the Past 3, 527–540.

Loulergue, L., Schilt, A., Spahni, R., Masson-Delmotte, V., Blunier, T., Lemieux, B., Barnola, J.M., Raynaud, D., Stocker, T.F., Chappellaz, J., 2008. Orbital and millennial-scale features of atmospheric CH4 over the past 800,000 years. Nature 453, 383–386.

McManus, J.F., Oppo, D.W., Cullen, J.L., 1999. A 0.5-Million-Year Record of the millennial-scale climate variability in the North Atlantic. Science 283, 971–975.

NorthGRIP-community-members, 2004. High-resolution record of Northern Hemisphere climate extending into the last interglacial period. Nature 431, 147–151.

Paillard, D., Labeyrie, L., Yiou, P., 1996. Macintosh program performs time-series analysis. EOS, Transactions, American Geophysical Union 77 (39), 379.

Parrenin, F., Barnola, J.M., Beer, J., Blunier, T., Castellano, E., Chappellaz, J., Dreyfus, G., Fischer, H., Fujita, S., Jouzel, J., Kawamura, K., Lemieux-Dudon, B., Loulergue, L., Masson-Delmotte, V., Narcisi, B., Petit, J.R., Raisbeck, G., Raynaud, D., Ruth, U., Schwander, J., Severi, M., Spahni, R., Steffensen, J.P., Svensson, A., Udisti, R., Waelbroeck, C., Wolff, E., 2007. The EDC3 chronology for the EPICA Dome C ice core. Climate of the Past 3, 485–497.

Petit, J.R., Jouzel, J., Raynaud, D., Barkov, N.I., Barnola, J.M., Basile, I., Bender, M., Chappellaz, J., Davis, M., Delaygue, G., Delmotte, M., Kotlyakov, V.M., Legrand, M., Lipenkov, V.Y., Lorius, C., Pepin, L., Ritz, C., Saltzman, E., Stievenard, M., 1999. Climate and atmospheric history of the past 420,000 years from the Vostok ice core, Antarctica. Nature 399, 429–436.

Raisbeck, G.M., Yiou, F., Jouzel, J., Stocker, T.F., 2007. Direct north-south synchronization of abrupt climate change record in ice cores using Beryllium 10. Climate of the Past 3, 541–547.

Ruth, U., Barnola, J.M., Beer, J., Bigler, M., Blunier, T., Castellano, E., Fischer, H., Fundel, F., Huybrechts, P., Kaufmann, P., Kipfstuhl, S., Lambrecht, A., Morganti, A., Oerter, H., Parrenin, F., Rybak, O., Severi, M., Udisti, R., Wilhelms, F., Wolff, E., 2007. "EDML1": a chronology for the EPICA deep ice core from Dronning Maud Land, Antarctica, over the last 150 000 years. Climate of the Past 3, 475–484.

Schwander, J., Sowers, T., Barnola, J.M., Blunier, T., Fuchs, A., Malaizé, B., 1997. Age scale of the air in the summit ice: implication for glacial-interglacial temperature change. Journal of Geophysical Research 102, 19483–19493.

Severi, M., Becagli, S., Castellano, E., Morganti, A., Traversi, R., Udisti, R., Ruth, U., Fischer, H., Huybrechts, P., Wolff, E., Parrenin, F., Kaufmann, P., Lambert, F., Steffensen, J.P., 2007. Synchronisation of the EDML and EDC ice cores for the last 52 kyr by volcanic signature matching. Climate of the Past 3, 367–374.

Severinghaus, J., Beaudette, R., Headly, M.A., Taylor, H., Brook, E.J., 2009. Oxygen-18 of O_2 records the impact of abrupt climate change on the terrestrial biosphere. Science 324, 1431–1434.

Severinghaus, J.P., Sowers, T., Brook, E.J., Alley, R.B., Bender, M.L., 1998. Timing of abrupt climate change at the end of the Younger Dryas interval from thermally fractionated gases in polar ice. Nature 391, 141–146.

Severinghaus, J.P., Grachev, A., Battle, M., 2001. Thermal fractionation of air in polar firn by seasonal temperature gradients. Geochemistry Geophysics Geosystems 2 2000GC000146.

Severinghaus, J.P., Brook, E.J., 1999. Abrupt climate change at the end of the last glacial period inferred from trapped air in polar ice. Science 286, 930–934.

Severinghaus, J.P., Battle, M.O., 2006. Fractionation of gases in polar lee during bubble close-off: new constraints from firn air Ne, Kr and Xe observations. Earth and Planetary Science Letters 244, 474–500.

Shackleton, N.J., 2000. The 100,000-year ice-age cycle identified and found to lag temperature, carbon dioxide, and orbital eccentricity. Science 289, 1897–1902.

Sowers, T., Bender, M., Raynaud, D., Korotkevich, Y.S., 1992. $\delta^{15}N$ of N_2 in air trapped in polar ice: a tracer of gas transport in the firn and a possible constraint on ice age-gas differences. Journal of Geophysical Research 97, 15,683–15,697.

Sowers, T., Bender, M., Labeyrie, L., Martinson, D., Jouzel, J., Raynaud, D., Pichon, J.J., Korotkevich, Y.S., 1993. A 135,000-year Vostok-Specmap common temporal framework. Paleoceanography 8, 737–766.

Spahni, R., Schwander, J., Flückiger, J., Stauffer, B., Chappellaz, J., Raynaud, D., 2003. The attenuation of fast atmospheric CH_4 variations recorded in polar ice cores. Geophysical Research Letters 30, 1571. doi:10.1029/2003GL17093.

Spahni, R., Chappellaz, J., Stocker, T.F., Loulergue, L., Hausammann, G., Kawamura, K., Flückiger, J., Schwander, J., Raynaud, D., Masson-Delmotte, V., Jouzel, J., 2005. Atmospheric methane and nitrous oxide of the late Pleistocene from Antarctic ice cores. Science 310, 1317–1321.

Stenni, B., Selmo, E., Masson-Delmotte, V., Oerter, H., Meyer, H., Rothlisberger, R., Jouzel, J., Cattani, O., Falourd, S., Fischer, H., Hoffmann, G., Lacumin, P., Johnsen, S.J., Minster, B., 2010. The deuterium excess records of EPICA Dome C and Dronning Maud Land ice cores (East Antarctica). Quaternary Science Reviews 29, 146–159.

Stocker, T.F., Johnsen, S.J., 2003. A minimum thermodynamic model for the bipolar seesaw. Paleoceanography 18, 1087.

Suwa, M., Bender, M.L., 2008. O_2/N_2 ratios of occluded air in the GISP2 ice core. Journal of Geophysical Research 113, D11119. doi:10.1029/2007JD009589.

Svensson, A., Andersen, K.K., Bigler, M., Clausen, H.B., Dahl-Jensen, D., Davies, S.M., Johnsen, S.J., Muscheler, R., Parrenin, F., Rasmussen, S.O., Röthlisberger, R., Seierstad, I., Steffensen, J.P., Vinther, B.M., 2008. A 60 000 year Greenland stratigraphic ice core chronology. Climate of the Past 4, 47–57.

Voelker, A.H.L., 2002. Global distribution of centennial-scale records for Marine Isotope Stage (MIS) 3: a database. Quaternary Science Reviews 21, 1185–1212.

Waelbroeck, C., Labeyrie, L., Michel, E., Duplessy, J.C., McManus, J.F., Lambeck, K., Balbon, E., Labracherie, M., 2002. Sea-level and deep water temperature changes derived from benthic foraminifera isotopic records. Quaternary Science Reviews 21, 295–305.

Wang, Y., Cheng, H., Edwards, R.L., Kong, X., Shao, X., Chen, S., Wu, J., Jiang, X., Wang, X., An, Z., 2008. Millennial- and orbital-scale changes in the East Asian monsoon over the past 224,000 years. Nature 451, 1090–1093.

Yiou, F., Raisbeck, G.M., Baumgartner, S., Beer, J., Hammer, C., Johnsen, S., Jouzel, J., Kubik, P.W., Lestringuez, J., Stievenard, M., Suter, M., Yiou, P., 1997. Beryllium 10 in the Greenland Ice Core Project ice core at Summit, Greenland. Journal of Geophysical Research 102, 26783–26794.